



# Correlations between 14-gene RNA-level assay and clinical and molecular features in resectable non-squamous non-small cell lung cancer: a cross-sectional study

Zhicheng Huang<sup>1#</sup>, Ming Zhao<sup>2#</sup>, Bowen Li<sup>1#</sup>, Jianchao Xue<sup>1#</sup>, Yadong Wang<sup>1</sup>, Daoyun Wang<sup>1</sup>, Chao Guo<sup>1</sup>, Yang Song<sup>1</sup>, Haochen Li<sup>1,3</sup>, Xiaoqing Yu<sup>1</sup>, Xinyu Liu<sup>1</sup>, Ruirui Li<sup>4</sup>, Jian Cui<sup>5</sup>, Zhe Feng<sup>6</sup>, Lan Su<sup>7</sup>, Ka Luk Fung<sup>8</sup>, Heqing Xu Rachel<sup>9</sup>, Kakeru Hisakane<sup>10</sup>, Atocha Romero<sup>11</sup>, Shanqing Li<sup>1</sup>, Naixin Liang<sup>1</sup>

<sup>1</sup>Department of Thoracic Surgery, Peking Union Medical College Hospital, Chinese Academy of Medical Sciences and Peking Union Medical College, Beijing, China; <sup>2</sup>Department of Thoracic Surgery, Chinese PLA General Hospital, Beijing, China; <sup>3</sup>School of Medicine, Tsinghua University, Beijing, China; <sup>4</sup>Department of Thoracic Surgery, Civic Aviation General Hospital, Beijing, China; <sup>5</sup>Department of Thoracic Surgery, Beijing Chuiyangliu Hospital Affiliated to Tsinghua University, Beijing, China; <sup>6</sup>Department of Thoracic Surgery, Beijing No. 6 Hospital, Beijing, China; <sup>7</sup>Burning Rock Biotech, Guangzhou, China; <sup>8</sup>Department of Pharmaceutical Chemistry, University of Toronto, Toronto, Canada; <sup>9</sup>Department of Faculty of Social Sciences and Law, University of Bristol, Bristol, UK; <sup>10</sup>Department of Pulmonary Medicine and Oncology, Graduate School of Medicine, Nippon Medical School, Tokyo, Japan; <sup>11</sup>Medical Oncology Department, Hospital Universitario Puerta de Hierro de Majadahonda, Madrid, Spain

**Contributions:** (I) Conception and design: N Liang, Z Huang, M Zhao; (II) Administrative support: S Li, N Liang; (III) Provision of study materials or patients: N Liang, M Zhao; (IV) Collection and assembly of data: J Xue, Y Wang, D Wang, C Guo, Y Song, H Li, X Yu, X Liu, R Li, J Cui, Z Feng, KL Fung, HX Rachel; (V) Data analysis and interpretation: Z Huang, B Li, J Xue, L Su; (VI) Manuscript writing: All authors; (VII) Final approval of manuscript: All authors.

<sup>#</sup>These authors contributed equally to this work.

**Correspondence to:** Naixin Liang, MD. Department of Thoracic Surgery, Peking Union Medical College Hospital, Chinese Academy of Medical Sciences and Peking Union Medical College, No. 1 Shuaifuyuan Wangfujing, Dongcheng District, Beijing 100730, China. Email: pumchnelson@163.com.

**Background:** Non-small cell lung cancer (NSCLC) is the leading cause of cancer-related death worldwide. Accurate risk stratification is essential for optimizing treatment strategies. A 14-gene RNA-level assay of lung cancer, which involves quantitative reverse transcription polymerase chain reaction (qRT-PCR) analysis of formalin-fixed paraffin-embedded (FFPE) tissue samples, offers a promising approach. The aim of our study was to assess the relationships between risk stratification, as determined by a 14-gene RNA-level assay, and various clinical and molecular characteristics.

**Methods:** We retrospectively collected the preoperative clinical information and molecular testing information from 102 resectable non-squamous NSCLC patients. The 14-gene RNA-level assay was performed by extracting RNA from FFPE samples, followed by reverse transcription and quantification via quantitative polymerase chain reaction (qPCR) to assess the expression levels of 11 cancer-associated genes and three housekeeping genes. These gene expression levels were used to calculate a risk score, enabling patient stratification into distinct risk groups. Based on the 14-gene risk stratification, we analyzed the correlations between the clinical and molecular characteristics across the high-, medium-, and low-risk groups.

**Results:** A total of 102 patients were included in the study. The mean age was 55.19 years, 67 (65.7%) patients were female, and 18 (17.6%) had a smoking history. The 14-gene risk stratification classified patients into low-risk (n=63), intermediate-risk (n=25), and high-risk (n=14) groups. No significant differences were observed in baseline demographics between the three risk groups. High-risk patients had significantly higher mean computed tomography (CT) value ( $P=0.01$ ) and enhanced CT value ( $P=0.02$ ) compared to low-risk

<sup>^</sup> ORCID: 0000-0003-0399-9668.

patients. Genomic profiling of 89 patients revealed specific mutations that were significantly associated with the higher-risk groups. Tumor mutational burden (TMB) was higher in higher-risk groups ( $P=0.007$ ). In clinically low-risk patients ( $n=85$ ) as recognized by the NCCN guidelines, the 14-gene risk stratification model reclassified 30 out from the 85 clinically low-risk patients, with 19 placed in the medium-risk group and 11 in the high-risk group, while the remaining samples were still classified as low-risk. Additionally, we found that three patients who were not recommended for adjuvant therapy by the Multiple-gene INdex to Evaluate the Relative benefit of Various Adjuvant therapies (MINERVA) model were classified as high risk and 13 as intermediate risk.

**Conclusions:** Our results indicate that 14-gene RNA-level assay is correlated with specific genetic mutations, including *TP53*, *KRAS*, and *LRP1B*. These insights provide a stronger foundation for integrating molecular risk assessment with clinical and imaging data, offering more comprehensive information to guide more targeted and effective adjuvant therapy strategies in the future management of lung cancer.

**Keywords:** Risk stratifications; 14-gene RNA-level assay; non-squamous non-small cell lung cancer (non-squamous NSCLC)

Submitted Oct 07, 2024. Accepted for publication Nov 14, 2024. Published online Nov 27, 2024.

doi: 10.21037/tlcr-24-913

View this article at: <https://dx.doi.org/10.21037/tlcr-24-913>

## Introduction

Lung cancer is the leading cause of cancer-related death in China and the world, contributing significantly to the overall cancer burden (1). Non-small cell lung cancer (NSCLC) accounts for the majority (approximately 85%)

of lung cancer cases, presenting various management and prognostic challenges. Lung adenocarcinoma (LUAD) is the most common histological subtype of NSCLC, accounting for 40% of lung malignancies (2). Early surgical resection currently serves as the standard treatment for patients with early-stage NSCLC. The postoperative prognosis of patients influenced by multiple factors. Evaluating whether patients require postoperative adjuvant therapy is crucial for improving outcomes. Several risk stratification systems have been implemented to predict the prognosis of patients with lung cancer, incorporating clinical, histopathological, molecular, or integrated factors (3-5). Examples include the National Comprehensive Cancer Network (NCCN) high-risk factors, tumor-node-metastasis (TNM) staging system, and molecular residual disease (MRD) assessment (6,7). According to the NCCN guidelines, all stage IA patients and selected stage IB patients without risk factors do not need to receive adjuvant therapy (8). However, in clinical practice, some patients with early-stage lung cancer categorized as low risk still experience postoperative recurrence and metastasis, as stage I patients have a 5-year survival rate ranging from 68% to 92% (9). This indicates that traditional risk stratification systems have limitations and cannot comprehensively reflect tumor characteristics.

The 14-gene risk stratification of lung cancer incorporates 11 cancer-related target genes and three reference genes. The assay uses quantitative reverse transcription polymerase chain reaction (qRT-PCR) to analyze formalin-fixed

### Highlight box

#### Key findings

- The 14-gene risk stratification assay demonstrated a closer association with molecular characteristics than traditional risk stratification methods and thus may offer more precise patient stratification at the molecular level.
- Higher computed tomography value correlate with increased risk, indicating that higher nodule solidity is associated with higher 14-gene risk stratification.

#### What is known and what is new?

- Traditional risk stratification systems for lung cancer have limitations in accurately predicting patient outcomes.
- Based on the 14-gene risk stratification, we analyzed the correlations between the clinical and molecular characteristics across the high-, medium-, and low-risk groups.

#### What is the implication, and what should change now?

- Independent of traditional clinical, pathological, and molecular markers, the 14-gene risk stratification provides RNA-level insights into risk stratification for non-squamous non-small cell lung cancer patients.

paraffin-embedded (FFPE) tissue samples, which are readily available and highly stable (10). It is designed for precise risk stratification of recurrence in patients with early-stage non-squamous NSCLC and for predicting the benefits of postoperative adjuvant therapy. The 14-gene risk stratification encompasses a variety of crucial processes that are not reflected by current clinical indicators, such as apoptosis, DNA repair, cell cycle regulation, cell proliferation and survival, cell migration and invasion, immune cell regulation, and key signaling pathways (11-13). The assay was initially developed at the University of California San Francisco (UCSF) using a training cohort of samples from 361 patients with non-squamous NSCLC, and calculates a risk score based on the expression of the 14 genes and stratifies patients with lung cancer treated with surgical resection into low-, medium-, and high-mortality risk categories (10,14).

The Kaiser Permanente Division of Research evaluated the prognostic impact of this risk stratification on stage I non-squamous NSCLC patients, demonstrating significant differences in 5-year overall survival (OS) among the low-, medium-, and high-risk groups based on the 14-gene risk stratification, the high-risk group was associated with worse prognosis (10). Additionally, some studies indicated that the 14-gene RNA-level assay can predict recurrence in early-stage NSCLC, with a significant difference in 5-year disease-free survival (DFS) between the low-risk and high-risk groups (15). Among stage I-IIA patients, high-risk individuals may benefit from adjuvant therapy (16). Therefore, the 14-gene RNA-level assay demonstrated the ability to improve upon the existing risk categories set by NCCN.

Although previous studies have demonstrated the prognostic utility of the 14-gene risk stratification model in both Western and Chinese populations, the associations between the 14-gene risk groups and detailed clinical, radiological, and genetic characteristics, as well as the concordance and differences between this model and traditional risk stratification approaches, remain unclear. Here, we present real-world data from 102 postoperative patients across two clinical centers in China. Comprehensive clinical information, along with imaging and DNA-level next-generation sequencing (NGS) analyses, was collected for all samples. Based on the 14-gene risk stratification, we analyzed the correlations between clinical and molecular characteristics across the high-, intermediate-, and low-risk groups. We present this article in accordance with the STROBE reporting checklist (available at <https://tldr.amegroups.com/article/view/10.21037/tldr-24-913/rc>).

## Methods

### *Study population*

We included a total of 102 patients with resectable non-squamous NSCLC who had undergone radical resection at the Peking Union Medical College Hospital and Chinese PLA General Hospital between 2020 and 2022. All patients had their tissue samples subjected to molecular risk stratification by the 14-gene prognostic assay, which involves qRT-PCR analysis of FFPE tissue samples. And genomic profiling was performed using NGS. For each patient, we retrospectively collected preoperative clinical information, including gender, age, smoking history, pathological subtype, pathological stage, maximum standardized uptake value (SUVmax), imaging findings, etc. The study was conducted in accordance with the Declaration of Helsinki (as revised in 2013). The study was approved by the ethics committee of Peking Union Medical College Hospital (No. K4171) and informed consent was taken from all the patients. Chinese PLA General Hospital was informed and agreed with this study.

### *Risk stratification using a 14-gene assay*

Total RNA was isolated from FFPE samples using the RNeasy FFPE Kit (Qiagen, Hilden, Germany), following the manufacturer's guidelines. Extraction yield (ng) and RNA purity (A260/280 and A260/230 ratios) were measured with a Nanodrop spectrophotometer (Thermo Fisher Scientific, Waltham, MA, USA). The RNA was then reverse-transcribed into cDNA, followed by quantitative polymerase chain reaction (qPCR) using TaqMan assays, as previously described (17). Specifically, we quantified the expression levels of 11 cancer-associated genes (*BAG1*, *BRCA1*, *CDC6*, *CDK2AP1*, *ERBB3*, *FUT3*, *IL11*, *LCK*, *RND3*, *SH3BGR*, *WNT3A*) and three housekeeping genes (*ESD*, *TBP*, *YAP1*). Relative expression for each gene was calculated using the comparative cycle threshold (Ct) method. Based on the expression levels of the 11 target genes, a continuous risk score was generated for each individual using a pre-established model. Patients were then categorized into low-, medium-, and high-risk groups according to predetermined cutoffs and risk scores (10).

### *DNA isolation and capture-based targeted DNA sequencing*

DNA isolation and targeted sequencing were conducted at the College of American Pathologists (CAP)-accredited and

Clinical Laboratory Improvement Amendments (CLIA)-certified laboratory of Burning Rock Biotech (Guangzhou, China). The main experimental workflow included several key steps (17,18). Firstly, tumor DNA was extracted from FFPE samples using the QIAamp DNA FFPE Tissue Kit (Qiagen). Subsequently, the extracted DNA was sheared into 200–400 bp fragments and purified using the Agencourt AMPure XP Kit (Beckman Coulter, Brea, CA, USA). Next, target capture was performed using a commercial 520-gene panel (OncoScreen Plus, Burning Rock Biotech), which covered 1.86 megabases of the human genome. The DNA fragments were hybridized with capture probe baits, followed by magnetic bead selection and amplification. Following this, the quality and size of the DNA fragments were evaluated using a High Sensitivity DNA Kit with the Bioanalyzer 2100 (Agilent Technologies, Santa Clara, CA, USA). The indexed samples were then subjected to paired-end sequencing using the Illumina NextSeq 500 system (San Diego, CA, USA), with an average sequencing depth of 1,000× for tumor tissue samples. Finally, leukocyte DNA served as the germline control and was processed using the same methods as tumor DNA, with a sequencing depth of 300×.

### *Analysis of sequence data*

The genomic analysis workflow for cancer samples was conducted by first aligning sequence data to the reference human genome (hg19) using the Burrows-Wheeler Aligner (BWA) version 0.7.10. (19). Local realignment, duplicate marking, and somatic variant calling were subsequently performed using Genome Analysis Tool Kit (GATK) version 3.2 and VarScan version 2.4.3, with leukocyte DNA used as a matched normal control to distinguish somatic mutations from germline variants (20,21). Variants were then filtered using the VarScan ffilter pipeline, with loci having a read depth of less than 100 removed. For tissue samples, single nucleotide variants (SNVs) required at least 8 supporting reads, while insertions and deletions (Indels) required 2 and 5 supporting reads, respectively. Variants with a population frequency greater than 0.1% in the ExAC, 1000 Genomes, dbSNP, or ESP6500SI-V2 databases were classified as single nucleotide polymorphisms (SNPs) and excluded from further analysis. The remaining variants were annotated using ANNOVAR (release dated February 1, 2016) and SnpEff version 3.6. Structural variants (SVs) were analyzed using Facter version 1.4.3, and copy number variations (CNVs) were assessed based on the depth of coverage across captured intervals, correcting for sequencing bias due to GC

content and probe design. Coverage data were normalized across samples to comparable scales by using the average coverage of all capture regions. CNV determination was made by calculating the ratio of the tumor sample's depth of coverage to the average coverage across an adequate number ( $n > 50$ ) of control samples without CNVs for each captured interval, with regions showing significant quantitative and statistical differences compared to controls designated as CNVs. CNV thresholds were set at 1.5 for deletions and 2.64 for amplifications. The microsatellite instability (MSI) status of tumor samples was determined using a previously established read count distribution-based method (22,23).

### *Calculation of tumor mutational burden (TMB)*

TMB is determined by calculating the ratio between the total number of detected nonsynonymous mutations and the size of the panel's coding region. The mutations counted include nonsynonymous SNVs and indels found within the coding regions, as well as within the upstream or downstream  $\pm 2$  base pair regions. It excluded hot mutation events, CNVs, SVs, and germline SNPs. Only mutations with an allele frequency (AF) of at least 2% are included in the TMB calculation. Additionally, the maximum AF (maxAF) in tissue samples must be at least 5% to ensure adequate sample quality. TMB is computed using the following formula:

$$\text{TMB} = \frac{\text{mutation count (except for CNV, SV, SNPs, and hot mutations)}}{\text{coding region size}} \quad [1]$$

### *Statistical analysis*

The statistical analyses were conducted using R version 4.2.3 (The R Foundation for Statistical Computing, Vienna, Austria). Categorical variables with multiple groups, such as pathological subtypes or staging, were analyzed using the Fisher exact test. The Kruskal-Wallis test was used to test for differences in continuous variables, such as age, maximum tumor diameter (MTD), computed tomography (CT) value, and SUVmax, when risk groups were divided into three or more groups. When risk groups were divided into two groups, the Wilcoxon rank-sum test was used instead. The P value of less than 0.05 was considered indicative of a statistically significant difference.

The relationship between risk score and CT value, SUVmax, MTD, and TMB was evaluated using the `cor.test()` function in R. The choice of correlation coefficient was determined based on the distributional characteristics of the variables. Pearson correlation coefficients were used for variables with

**Table 1** Clinical and pathological characteristics of patients with different risk stratifications

Characteristics	Low risk	Medium risk	High risk	Overall	Significance
Total	63	25	14	102	
Sex					NS
Male	18 (28.6)	9 (36.0)	8 (57.1)	35 (34.3)	
Female	45 (71.4)	16 (64.0)	6 (42.9)	67 (65.7)	
Age (years)	54.08	58.92	53.29	55.19	NS
Smoking history					NS
Yes	7 (11.1)	6 (24.0)	5 (35.7)	18 (17.6)	
No	52 (82.5)	19 (76.0)	9 (64.3)	80 (78.4)	
Unknown	4 (6.3)	0 (0.0)	0 (0.0)	4 (3.9)	
Pulmonary fibrosis					NS
Yes	1 (1.6)	0 (0.0)	1 (7.1)	2 (2.0)	
No	62 (98.4)	25 (100.0)	13 (92.9)	100 (98.0)	
COPD					NA
No	63 (100.0)	25 (100.0)	14 (100.0)	102 (100.0)	
TB					NS
Yes	0 (0.0)	0 (0.0)	1 (7.1)	1 (1.0)	
No	63 (100.0)	25 (100.0)	13 (92.9)	101 (99.0)	
Stage					NS
AAH	1 (1.6)	0 (0.0)	0 (0.0)	1 (1.0)	
AIS	5 (7.9)	0 (0.0)	1 (7.1)	6 (5.9)	
IA1	19 (30.2)	5 (20.0)	3 (21.4)	27 (26.5)	
IA2	21 (33.3)	10 (40.0)	4 (28.6)	35 (34.3)	
IA3	10 (15.9)	3 (12.0)	1 (7.1)	14 (13.7)	
IB	7 (11.1)	6 (24.0)	3 (21.4)	16 (15.7)	
IIB	0 (0.0)	0 (0.0)	1 (7.1)	1 (1.0)	
IIIA	0 (0.0)	1 (4.0)	1 (7.1)	2 (2.0)	

Data are expressed as n, n (%), or mean. NS, no significance; COPD, chronic obstructive pulmonary disease; NA, not applicable; TB, tuberculosis; AAH, atypical adenomatous hyperplasia; AIS, adenocarcinoma in situ.

a normal distribution, Spearman correlation coefficients were used for variables with a nonnormal distribution. The plots were created using the “ggplot2” package in R.

## Results

### Patient characteristics

A total of 102 patients were included in the study (Table 1).

The mean age was 55.19 years, 67 (65.7%) patients were female, and 18 (17.6%) had a smoking history. The majority of patients (n=76, 74.4%) were diagnosed with stage IA adenocarcinoma, one patient had atypical adenomatous hyperplasia (AAH), six patients had adenocarcinoma in situ (AIS), one had stage IIB disease, and two had stage IIIA disease. The 14-gene prognostic assay classified 63 patients as low risk, 25 as intermediate risk, and 14 as high risk.



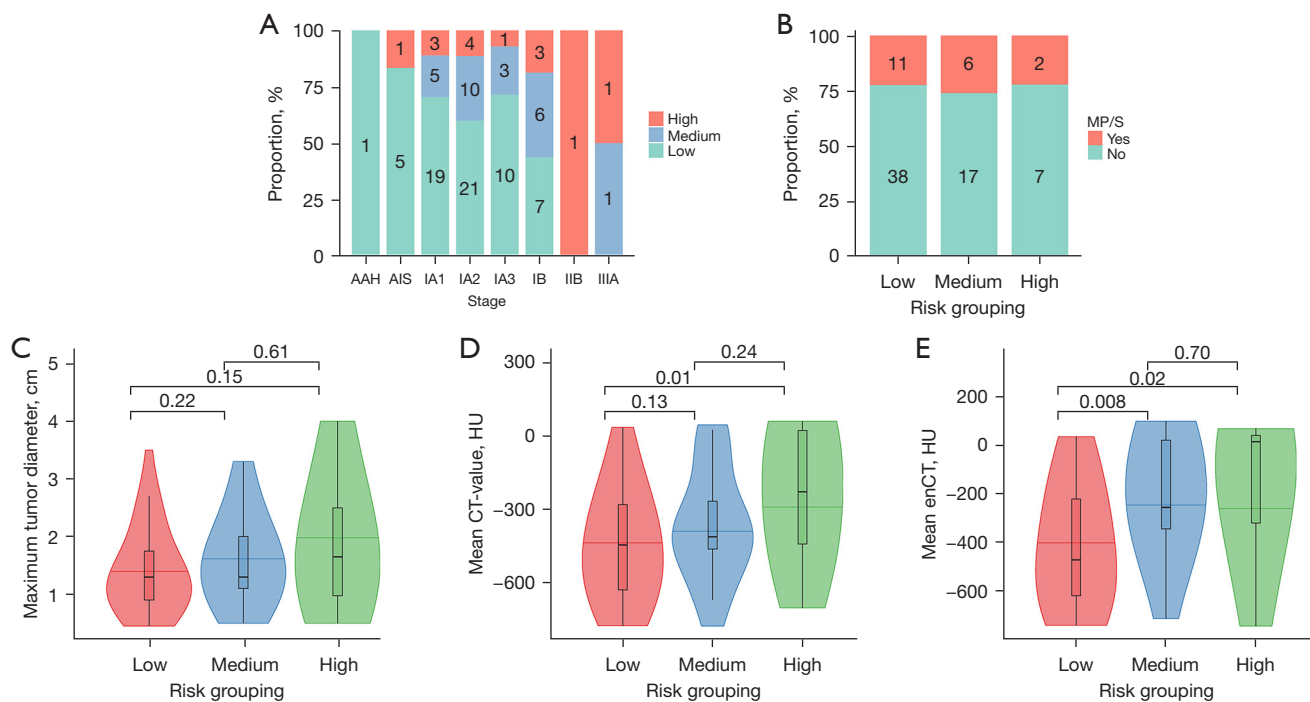


**Figure 1** The relationship between risk groups and clinical characteristics. (A) A stacked bar chart, depicting the relationship between risk stratification and TNM staging. (B) The association between risk stratification and the presence or absence of pathological MP/S types. (C) A violin plot depicting the relationship between risk stratification and MTD. (D) A violin plot depicting the association between risk stratification and the average CT value. (E) A violin plot depicting the relationship between risk stratification and the average enhanced CT value. AAH, atypical adenomatous hyperplasia; AIS, adenocarcinomas in situ; MP/S, micropapillary or solid; CT, computed tomography; HU, Hounsfield unit; enCT, enhanced CT; TNM, tumor-node-metastasis; MTD, maximum tumor diameter.

### Correlation of clinical and pathological characteristics with the 14-gene risk stratification

We did not observe significant differences in age, sex, smoking history-, family tumor history, or other benign pulmonary diseases between the three risk groups (Table 1). Regarding pathological features, the 14-gene risk stratification revealed no significant association with TNM staging, pathological subtype, or the presence of micropapillary or solid (MP/S) subtype ( $P=0.94$ ) (Figure 1A,1B). No correlation was observed between risk stratification and MTD (Figure 1C). Patients classified as high risk showed a significantly higher mean CT value ( $P=0.01$ ), reflecting the solidity of pulmonary nodules, compared with low-risk patients (Figure 1D). Similarly, high- and medium-risk patients also showed significantly higher mean enhanced CT value than did low-risk patients ( $P=0.02$  and  $P=0.008$ , respectively) (Figure 1E). The SUVmax as assessed by  $^{18}\text{F}$ -fluorodeoxyglucose positron emission tomography-CT ( $^{18}\text{F}$ FDG-PET/CT) and reflecting intratumor cellular glucose metabolic activity did not show significant

differences between the three risk groups (Figure S1). Additionally, the 14-gene prognostic assay generated a raw score, and we conducted correlation analyses between the raw risk score and various clinical characteristics. We found significant statistical correlations between the risk score and MTD, mean CT value, maximum CT value, enhanced CT value, SUVmax, and TMB (Figure 2).

### Relevance between risk stratification and molecular features

Genomic profiling also was conducted for 89 patients in the cohort. *EGFR* ( $n=62$ , 70%) was the most frequently mutated gene, followed by *TP53* ( $n=26$ , 29%). To analyze the association between these mutations and risk stratification, we selected the 10 genes with the highest mutation frequencies, excluding genes with synonymous mutations and classic driver mutations in lung cancer. The molecular risk stratification had a significant association with *TP53* mutations ( $P=0.03$ ), *KRAS* mutations ( $P=0.005$ ),

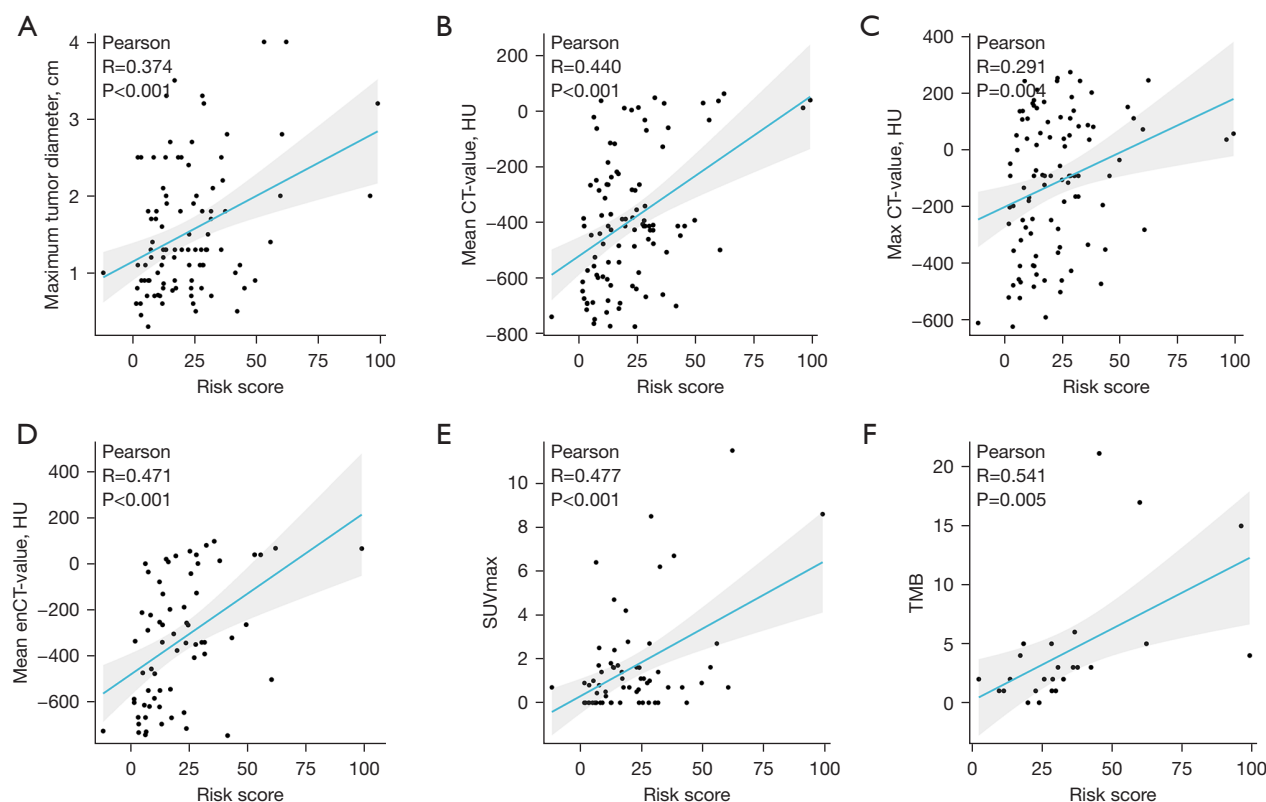


**Figure 2** A scatter plot showing the correlation between different clinical features and risk scores. (A) The correlation between risk scores and the MTD. (B) The correlation between risk scores and mean CT value. (C) The correlation between risk scores and maximum CT value. (D) The correlation between risk scores and mean enhanced CT value. (E) The correlation between risk scores and SUVmax. (F) The correlation between risk scores and TMB. CT, computed tomography; HU, Hounsfield unit; enCT, enhanced CT; SUVmax, maximum standardized uptake value; TMB, tumor mutational burden; MTD, maximum tumor diameter.

and *LRP1B* ( $P=0.03$ ) mutations but not with *EGFR* mutation ( $P=0.14$ ) (Figure 3). The TMB in the lower-risk group was significantly lower than that in the higher-risk group ( $P=0.007$ ) (Figure S1).

#### **Risk stratification among patients who do not require postoperative adjuvant therapy**

Eighty-five patients who did not qualify for adjuvant therapy based on current clinical consensus were categorized clinically low-risk group (Table 2). This group included all stage IA disease and stage IB patients without high-risk features as recognized by the NCCN guidelines, such as poorly differentiated tumors, vascular invasion, pleural invasion, and unknown lymph node status. However, the 14-gene risk stratification model reclassified 30 out from the 85 clinically low-risk patients, with 19 placed in the medium-risk group and 11 in the high-risk group, while

the remaining samples were still classified as low-risk.

We further investigated the differences among clinical, imaging, pathological, and molecular features according to risk groups. Our results showed that in the clinically low-risk group, solid nodules were more common in the high-risk group as assessed by the 14-gene prognostic assay ( $P=0.02$ ) (Figure 4A). Higher 14-gene risk levels were associated with increased mean CT values ( $P=0.02$ ) and mean enhanced CT values ( $P=0.02$ ) (Figure S2). Notably, no correlation was observed between risk stratification and MTD or SUVmax (Figure S2), which may indicate that these changes in early-stage lung cancer are not yet reflected in PET/CT imaging.

#### **Comparison of 14-gene risk stratification with the MINERVA model in EGFR-mutated patients**

The presence of *EGFR* mutation is a significant factor in

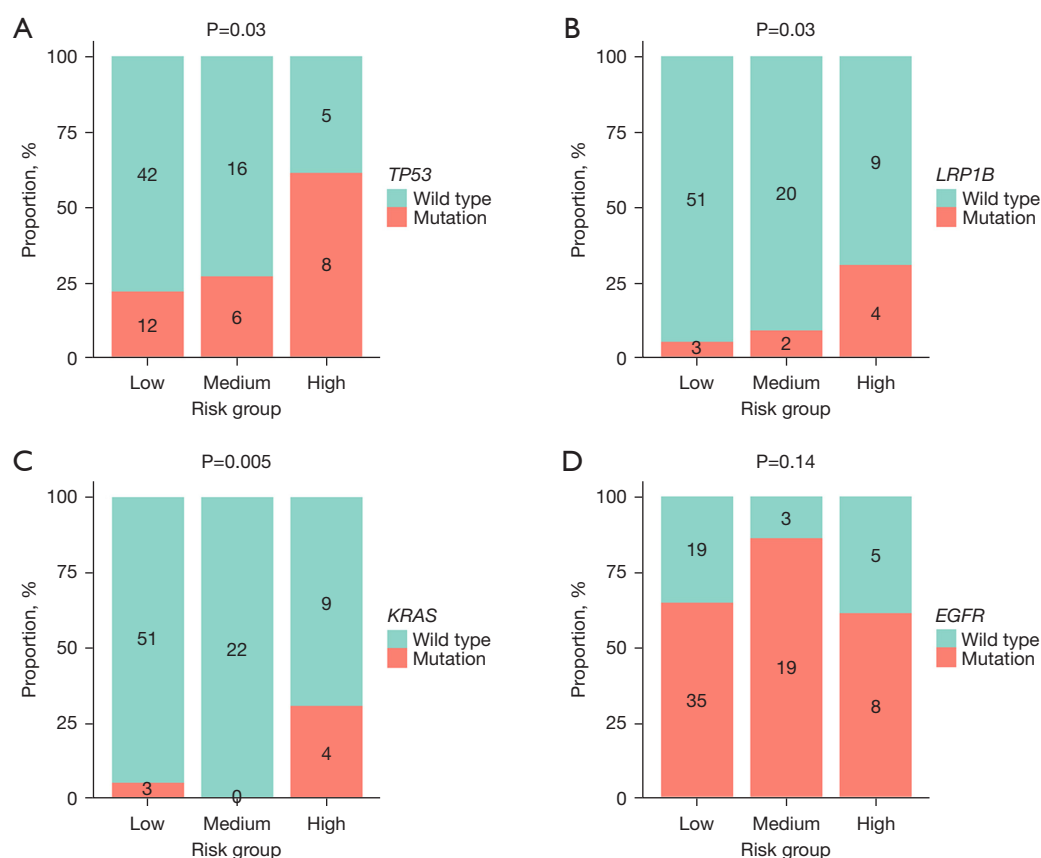


**Figure 3** The relationship between risk groups and molecular features. (A) A stacked bar chart depicting the association between risk stratification and the *TP53* mutation. (B) A stacked bar chart depicting the association between risk stratification and the *LRP1B* mutation. (C) A stacked bar chart depicting the association between risk stratification and the *KRAS* mutation. (D) A stacked bar chart depicting the association between risk stratification and the *EGFR* mutation.

guiding the choice of adjuvant therapy in clinical practice. In our study, 62 patients harbored *EGFR* mutations. Among them, 35 were classified as low risk by the 14-gene prognostic assay, 19 as medium risk, and eight as high risk. The Multiple-gene INdex to Evaluate the Relative benefit of Various Adjuvant therapies (MINERVA), a genomic signature-based predictive model derived from the ADJUVANT (CTONG1104) trial (24), can be used to guide the choice of adjuvant therapy (chemotherapy *vs.* targeted therapy) in resected patients with *EGFR*-mutant NSCLC. We stratified *EGFR*-mutant patients into chemotherapy (n=2), targeted therapy (n=16), and no adjuvant therapy (n=44) groups according to the NCCN guidelines and MINERVA scores. Among these, three patients classified as high risk and 13 patients as intermediate risk were not recommended for postoperative adjuvant therapy; meanwhile, seven patients classified as low risk were recommended for postoperative

adjuvant therapy (Figure 4B).

## Discussion

Our study investigated the correlation between 14-gene risk stratification and clinical and molecular characteristics, potentially aiding clinicians in formulating subsequent treatment strategies for patients.

Our results indicated no significant differences in basic demographic characteristics between the different risk groups, suggesting that the 14-gene risk stratification is not influenced by patients' baseline characteristics. Although pathological subtypes or TNM staging are often considered important prognostic indicators, Kratz *et al.* demonstrated that the 14-gene risk stratification has superior prognostic predictive value for patients with stage I–III NSCLC (10). Compared to the use of NCCN risk stratification and traditional



**Table 2** Characteristics of patients with different risk stratifications in the clinically low-risk group

Characteristics	Low risk	Medium risk	High risk	Overall	Significance
Total	55	19	11	85	
Sex					NS
Male	14 (25.5)	6 (31.6)	7 (63.6)	27 (31.8)	
Female	41 (74.5)	13 (68.4)	4 (36.4)	58 (68.2)	
Age (years)	54.33	59.89	53.55	55.47	NS
Smoking history					NS
Yes	7 (12.7)	3 (15.8)	4 (36.4)	14 (16.5)	
No	48 (87.3)	16 (84.2)	7 (63.6)	71 (83.5)	
Pulmonary fibrosis					NS
Yes	1 (1.8)	0 (0.0)	1 (9.1)	2 (2.4)	
No	54 (98.2)	19 (100.0)	10 (90.9)	83 (97.6)	
COPD					NA
No	55 (100.0)	19 (100.0)	11 (100.0)	85 (100.0)	
TB					NS
Yes	0 (0.0)	0 (0.0)	1 (9.1)	1 (1.2)	
No	55 (100.0)	19 (100.0)	10 (90.9)	84 (98.8)	
Stage					NS
AAH	1 (1.8)	0 (0.0)	0 (0.0)	1 (1.2)	
AIS	5 (9.1)	0 (0.0)	1 (9.1)	6 (7.1)	
IA1	17 (30.9)	5 (26.3)	3 (27.3)	25 (29.4)	
IA2	21 (38.2)	10 (52.6)	4 (36.4)	35 (41.2)	
IA3	9 (16.4)	3 (15.8)	1 (9.1)	13 (15.3)	
IB	2 (3.6)	1 (5.3)	2 (18.2)	5 (5.9)	

Data are expressed as n, n (%), or mean. NS, no significance; COPD, chronic obstructive pulmonary disease; NA, not applicable; TB, tuberculosis; AAH, atypical adenomatous hyperplasia; AIS, adenocarcinoma in situ.

TNM staging alone, the combined use of the 14-gene risk stratification enables the more accurate identification of prognostic risks. Similarly, our analysis showed no significant association between the 14-gene risk stratification and traditional pathological features such as TNM staging and histological subtypes. This indicates that the 14-gene risk stratification is independent of these traditional methods.

Additionally, we observed no statistically significant difference between risk stratification and tumor diameter. There was a correlation between risk stratification and radiological classification, with a higher proportion of mixed-solid ground-glass nodules and pure-solid nodules observed in the medium-to-high-risk group. This correlation suggests

that radiological features can support risk stratification, aiding in the early identification of more aggressive tumors and facilitating more proactive management of patients.

Regarding genetic characteristics, we found that *EGFR* mutation was not associated with the risk stratification determined by the 14-gene assay (25). The molecular profiling revealed significant correlations between the 14-gene assay risk groups and specific gene mutations, notably *TP53*, *KRAS*, and *LRP1B*, previous studies have reported that *TP53* and *KRAS* mutations were more prevalent in the high-risk group, supporting the notion that patients with these mutations have a poorer prognosis (26-28). Enhanced postoperative adjuvant therapy might potentially benefit patients with these gene

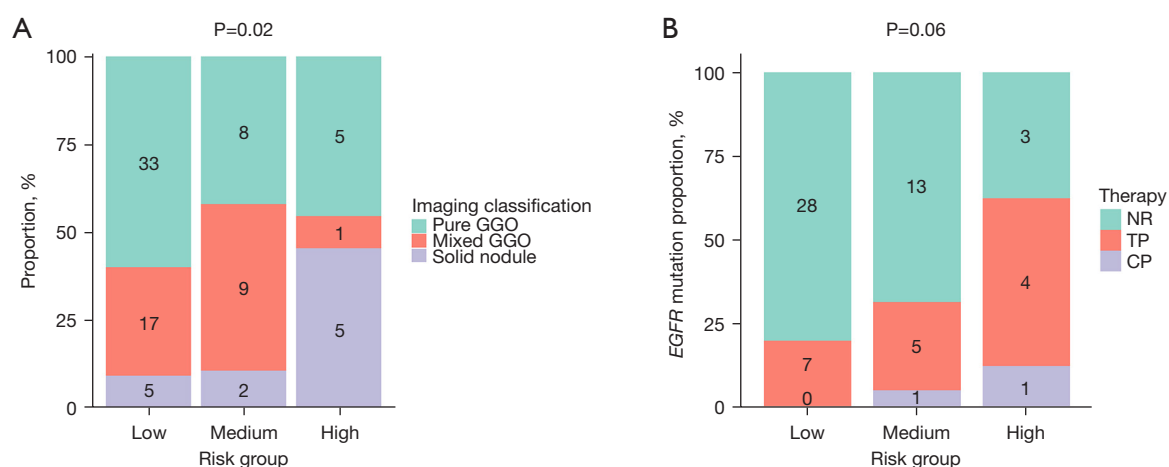


**Figure 4** The figure illustrates the relationship between 14-gene risk stratification with imaging classification in the clinically low-risk patients and the association between risk stratification and the postoperative adjuvant therapy recommended by MINERVA. (A) A stacked bar chart depicting the relationship between 14-gene risk stratification and imaging classification in the clinically low-risk group. (B) A stacked bar chart depicting the relationship between risk stratification and the postoperative adjuvant therapy recommended by MINERVA in the population with *EGFR* mutations. GGO, ground-glass opacity; NR, not recommended; TP, targeted therapy patients; CP, chemotherapy patients; MINERVA, Multiple-gene INDEX to Evaluate the Relative benefit of Various Adjuvant therapies.

mutations.

Additionally, in our study, some patients in the subgroup assessed as low risk by the NCCN were classified as intermediate or high risk. We found that three high-risk and 13 intermediate-risk patients classified by the 14-gene risk stratification were not recommended for adjuvant therapy by the MINERVA model. Previous large-scale study suggests that these patients might benefit from such treatment (10).

Our study involved several limitations which should be addressed. The brief follow-up period prevented us from accurately assessing recurrence statistics for these patients. Thus, the scope of this study was limited to the association between the 14-gene-based risk stratification and conventional clinical and genetic characteristics. We present these preliminary results to complement this 14-gene risk stratification model and to analyze the RNA-level risk stratification from a clinical standpoint. Once the authentic prognostic data mature, additional findings will be presented, and the RNA dimension assessment will be compared to other clinical or genetic prognostic models.

## Conclusions

Our results indicate that 14-gene RNA-level assay is correlated with specific genetic mutations, including *TP53*,

*KRAS*, and *LRP1B*. These insights provide a stronger foundation for integrating molecular risk assessment with clinical and imaging data, offering more comprehensive information to guide more targeted and effective adjuvant therapy strategies in the future management of lung cancer.

## Acknowledgments

We extend our gratitude to the Clinical Biobank (ISO 20387), Peking Union Medical College Hospital, Chinese Academy of Medical Sciences, for their valuable support in providing the samples.

**Funding:** This research was supported by grants from the Beijing Xisike-MSD Clinical Oncology Research Foundation (Nos. CSCO-Y-MSDPU2021-0190 and CSCO-Y-MSD2020-0270) and the National High-Level Hospital Clinical Research Funding (Nos. 2022-PUMCH-B-011 and 2022-PUMCH-A-106).

## Footnote

**Reporting Checklist:** The authors have completed the STROBE reporting checklist. Available at <https://tclr.amegroups.com/article/view/10.21037/tclr-24-913/rc>

**Data Sharing Statement:** Available at <https://tclr.amegroups.com>

[com/article/view/10.21037/tlcr-24-913/dss](https://doi.org/10.21037/tlcr-24-913/dss)

*Peer Review File:* Available at <https://tlcr.amegroups.com/article/view/10.21037/tlcr-24-913/prf>

*Conflicts of Interest:* All authors have completed the ICMJE uniform disclosure form (available at <https://tlcr.amegroups.com/article/view/10.21037/tlcr-24-913/coif>). L.S. is from Burning Rock Biotech. K.H. reports receiving personal fees from AstraZeneca, MSD, Kyorin Pharmaceutical, Chugai Pharmaceutical, and Daiichi-Sankyo, outside the submitted work. The other authors have no conflicts of interest to declare.

*Ethical Statement:* The authors are accountable for all aspects of the work in ensuring that questions related to the accuracy or integrity of any part of the work are appropriately investigated and resolved. The study was conducted in accordance with the Declaration of Helsinki (as revised in 2013). The study was approved by the ethics committee of Peking Union Medical College Hospital (No. K4171) and informed consent was taken from all the patients. Chinese PLA General Hospital was informed and agreed with this study.

*Open Access Statement:* This is an Open Access article distributed in accordance with the Creative Commons Attribution-NonCommercial-NoDerivs 4.0 International License (CC BY-NC-ND 4.0), which permits the non-commercial replication and distribution of the article with the strict proviso that no changes or edits are made and the original work is properly cited (including links to both the formal publication through the relevant DOI and the license). See: <https://creativecommons.org/licenses/by-nc-nd/4.0/>.

## References

- Han B, Zheng R, Zeng H, et al. Cancer incidence and mortality in China, 2022. *J Natl Cancer Cent* 2024;4:47-53.
- Comprehensive molecular profiling of lung adenocarcinoma. *Nature* 2014;511:543-50.
- Libling WA, Korn R, Weiss GJ. Review of the use of radiomics to assess the risk of recurrence in early-stage non-small cell lung cancer. *Transl Lung Cancer Res* 2023;12:1575-89.
- Merino K, Bassiri A, Parker B, et al. Predictive risk score for isolated brain metastasis in non-small cell lung cancer. *J Thorac Dis* 2024;16:3794-804.
- Wilk AM, Kozłowska E, Borys D, et al. Radiomic signature accurately predicts the risk of metastatic dissemination in late-stage non-small cell lung cancer. *Transl Lung Cancer Res* 2023;12:1372-83.
- Chen K, Zhao H, Shi Y, et al. Perioperative Dynamic Changes in Circulating Tumor DNA in Patients with Lung Cancer (DYNAMIC). *Clin Cancer Res* 2019;25:7058-67.
- Zhang JT, Liu SY, Gao W, et al. Longitudinal Undetectable Molecular Residual Disease Defines Potentially Cured Population in Localized Non-Small Cell Lung Cancer. *Cancer Discov* 2022;12:1690-701.
- Pignon JP, Tribodet H, Scagliotti GV, et al. Lung adjuvant cisplatin evaluation: a pooled analysis by the LACE Collaborative Group. *J Clin Oncol* 2008;26:3552-9.
- Li X, Fan F, Chen H. ASO Author Reflections: Long-Term Follow-Up Results of Stage IA Invasive Non-Small Cell Lung Cancer Patients. *Ann Surg Oncol* 2024;31:5772.
- Kratz JR, He J, Van Den Eeden SK, et al. A practical molecular assay to predict survival in resected non-squamous, non-small-cell lung cancer: development and international validation studies. *Lancet* 2012;379:823-32.
- Collard TJ, Urban BC, Patsos HA, et al. The retinoblastoma protein (Rb) as an anti-apoptotic factor: expression of Rb is required for the anti-apoptotic function of BAG-1 protein in colorectal tumour cells. *Cell Death Dis* 2012;3:e408.
- García-Rodríguez N, Domínguez-García I, Domínguez-Pérez MDC, et al. EXO1 and DNA2-mediated ssDNA gap expansion is essential for ATR activation and to maintain viability in BRCA1-deficient cells. *Nucleic Acids Res* 2024;52:6376-91.
- Wang F, Zhao F, Zhang L, et al. CDC6 is a prognostic biomarker and correlated with immune infiltrates in glioma. *Mol Cancer* 2022;21:153.
- Gupta AR, Woodard GA, Jablons DM, et al. Improved outcomes and staging in non-small-cell lung cancer guided by a molecular assay. *Future Oncol* 2021;17:4785-95.
- Kratz JR, Van den Eeden SK, He J, et al. A prognostic assay to identify patients at high risk of mortality despite small, node-negative lung tumors. *JAMA* 2012;308:1629-31.
- Woodard GA, Wang SX, Kratz JR, et al. Adjuvant Chemotherapy Guided by Molecular Profiling and Improved Outcomes in Early Stage, Non-Small-Cell Lung Cancer. *Clin Lung Cancer* 2018;19:58-64.
- Mao X, Zhang Z, Zheng X, et al. Capture-Based Targeted Ultradeep Sequencing in Paired Tissue and Plasma Samples Demonstrates Differential Subclonal ctDNA-Releasing Capability in Advanced Lung Cancer. *J Thorac*

- Oncol 2017;12:663-72.
18. Li YS, Jiang BY, Yang JJ, et al. Unique genetic profiles from cerebrospinal fluid cell-free DNA in leptomeningeal metastases of EGFR-mutant non-small-cell lung cancer: a new medium of liquid biopsy. *Ann Oncol* 2018;29:945-52.
  19. Li H, Durbin R. Fast and accurate short read alignment with Burrows-Wheeler transform. *Bioinformatics* 2009;25:1754-60.
  20. McKenna A, Hanna M, Banks E, et al. The Genome Analysis Toolkit: a MapReduce framework for analyzing next-generation DNA sequencing data. *Genome Res* 2010;20:1297-303.
  21. Koboldt DC, Zhang Q, Larson DE, et al. VarScan 2: somatic mutation and copy number alteration discovery in cancer by exome sequencing. *Genome Res* 2012;22:568-76.
  22. Zhu L, Huang Y, Fang X, et al. A Novel and Reliable Method to Detect Microsatellite Instability in Colorectal Cancer by Next-Generation Sequencing. *J Mol Diagn* 2018;20:225-31.
  23. Cai Z, Wang Z, Liu C, et al. Detection of Microsatellite Instability from Circulating Tumor DNA by Targeted Deep Sequencing. *J Mol Diagn* 2020;22:860-70.
  24. Liu SY, Bao H, Wang Q, et al. Genomic signatures define three subtypes of EGFR-mutant stage II-III non-small-cell lung cancer with distinct adjuvant therapy outcomes. *Nat Commun* 2021;12:6450.
  25. Jiang Y, Lin Y, Fu W, et al. The impact of adjuvant EGFR-TKIs and 14-gene molecular assay on stage I non-small cell lung cancer with sensitive EGFR mutations. *EClinicalMedicine* 2023;64:102205.
  26. Zhang Z, Xue J, Yang Y, et al. Influence of TP53 mutation on efficacy and survival in advanced EGFR-mutant non-small cell lung cancer patients treated with third-generation EGFR tyrosine kinase inhibitors. *MedComm (2020)* 2024;5:e586.
  27. Tsiouda T, Domvri K, Boutsikou E, et al. Prognostic Value of KRAS Mutations in Relation to PDL1 Expression and Immunotherapy Treatment in Adenocarcinoma and Squamous Cell Carcinoma Patients: A Greek Cohort Study. *J Pers Med* 2024;14:457.
  28. Parra ER, Zhang J, Duose DY, et al. Multi-omics Analysis Reveals Immune Features Associated with Immunotherapy Benefit in Patients with Squamous Cell Lung Cancer from Phase III Lung-MAP S1400I Trial. *Clin Cancer Res* 2024;30:1655-68.
- (English Language Editor: J. Gray)

**Cite this article as:** Huang Z, Zhao M, Li B, Xue J, Wang Y, Wang D, Guo C, Song Y, Li H, Yu X, Liu X, Li R, Cui J, Feng Z, Su L, Fung KL, Rachel HX, Hisakane K, Romero A, Li S, Liang N. Correlations between 14-gene RNA-level assay and clinical and molecular features in resectable non-squamous non-small cell lung cancer: a cross-sectional study. *Transl Lung Cancer Res* 2024;13(11):3202-3213. doi: 10.21037/tlcr-24-913